

See discussions, stats, and author profiles for this publication at: <https://www.researchgate.net/publication/45503950>

Electric-Field-Induced Local Layer Structure in Plasticized PVC Actuator

ARTICLE *in* THE JOURNAL OF PHYSICAL CHEMISTRY B · AUGUST 2010

Impact Factor: 3.3 · DOI: 10.1021/jp105239a · Source: PubMed

CITATIONS

6

READS

21

2 AUTHORS:



Hong Xia

Shinshu University, Ueda, Japan

14 PUBLICATIONS 51 CITATIONS

[SEE PROFILE](#)



Toshihiro Hirai

Shinshu University

197 PUBLICATIONS 1,459 CITATIONS

[SEE PROFILE](#)

Electric-Field-Induced Local Layer Structure in Plasticized PVC Actuator

Hong Xia and Toshihiro Hirai*

Smart Materials Engineering, Faculty of Textile and Technology, Shinshu University, 3-15-1 Tokida, Ueda, Nagano 386-8567, Japan

Received: June 7, 2010; Revised Manuscript Received: July 14, 2010

In order to investigate the molecular vibrations and structure variations of PVC gels with applied electric fields, a mechanical measurement (combined tensile and shear test) was proposed, and the Fourier transform infrared (FT-IR) spectrometry and in situ Raman spectroscopy were conducted to clarify the mechanism of electric-field-induced local layer structure in PVC gel and its relationship to gel creeping deformation. As a result, the electric-field-induced local layer structure and the migration of the solvent-rich phase in PVC gels were clarified. The layer of PVC gel clinging to the anode is softer than that near the cathode. The peaks of FT-IR spectra were shifted and changed in the gel surface on the anode and cathode. Using the in situ Raman spectroscopy, it is found that the intensity of the whole Raman spectra was reduced from the cathode to the anode, and the elastic modulus of the gel on the anode was smaller than that on the cathode. All of the results indicated that the electric field induced the local layer structure and caused the asymmetric actuation behavior in PVC gel actuators.

1. Introduction

Poly(vinyl chloride) (PVC) is a common and widely used polymer. Since PVCs can be easily mixed with a large amount of plasticizer to form gels, various properties of PVC gels have been investigated.^{1–3} However, the mechanism of PVC particle gelation and the structure of PVC gels are still the focus of much research. Marcilla et al. reported that PVC particles with a plasticizer formed a plastisol: the formation of PVC gel thus encompasses the steps liquid–sol–gel.⁴ The solvent penetrates into the PVC particles, dissolves grains, and stretches polymer chains. On addition of plasticizer, the PVC particles are swelled and glued together through a percolation process. When the solvent is completely evaporated at a moderate temperature, the PVC particles and plasticizer fuse to form a homogeneous gel.⁵ PVC gel is a physical gel with a three-dimensional network of cross-linked polymer chains.^{6–9} Li and Aoki el. made PVC/(DOP) gels and studied rheological images of PVC that included physical properties, structure, and sol–gel transition relations.^{10–12} Hong and Chu described the effects of phase separation on the structure of PVC,¹³ and one of the authors of the present paper found that PVC gel has unequal deformation on application of an electric field.^{14,15} This actuation appeared as an asymmetric creep motion on one side of the anode. Using different boundary conditions such as the shape and size of the gel and electrode, various PVC gel actuators can be designed. A bending actuator, variable focal length lens, rolling actuator, and finger actuator have been developed by our group.^{16–18} Moreover, PVC gel actuators are low cost, have low energy consumption, and are easily processed. As an actuator material, PVC gels exhibit superiority.

We have recently reported work on the deformation mechanism of PVC gels.^{19,20} It was found that PVC gel plasticized with dibutyl adipate (DBA) is strongly polarized in an external electrical field, and the intrinsic polarization charges accumulate on the gel surface near the anode. A force generated in the PVC gels was expected as the response of gel polarization, and it

mainly took place between the gel and the anode due to the accumulated negative charges on the surface of the PVC gel near the anode. This force caused asymmetric deformation of the PVC gel and resulted in creep along the anode. The magnitude of the deformation depended on the intensity of the applied electric field and the plasticizer content.

In the present work, in situ Raman and Fourier transform infrared (FT-IR) spectroscopy have been used to investigate the molecular vibrations and structure variations of PVC gels with applied electric fields. Mechanical measurements (combined shear and compressive test) were proposed to clarify the mechanism of electric-field-induced local layer structure in PVC gel and its relationship to gel creeping deformation.

2. Experimental Section

2.1. Materials. Five PVC gels were prepared with 10, 30, 50, 70, and 90 w/w% of plasticizer (DBA): the gels are denoted PVC10, PVC30, PVC 50, PVC70, and PVC90, respectively.

PVC (with degree of polymerization 3700) particles were blended with tetrahydrofuran (THF) as solvent and DBA as plasticizer for 3 days; then, the solution was transferred to a PTFE laboratory dish at room temperature. After 5 days of solvent evaporation, transparent PVC gel was formed. The thickness of all of the gel samples was approximately 0.5 mm.

2.2. Mechanical Measurements. The deformation process of PVC gel actuators is a complicated combination of stepwise deformation by creep and stress relaxation, and these phenomena cannot be easily distinguished. In order to better understand the status of gel actuation in an electric field, we utilized a thermal mechanical analyzer (TMA) and set up special units for mechanical measurements at room temperature.²¹ Figure 1 shows two setups for special shear and compressive tests. The gel sample was cut in a thin rectangular shape with thickness 0.5 mm and mounted in a tension clamp with insulating hard film (a) or a sample table (b), and then sandwiched between the electrodes (area = 6 × 5 mm² or φ = 10 mm) for application of an electric field with varying magnitude. For the special shear test, the PVC gels contact the aluminum electrodes with strong

* Corresponding author. E-mail: tohirai@shinshu-u.ac.jp

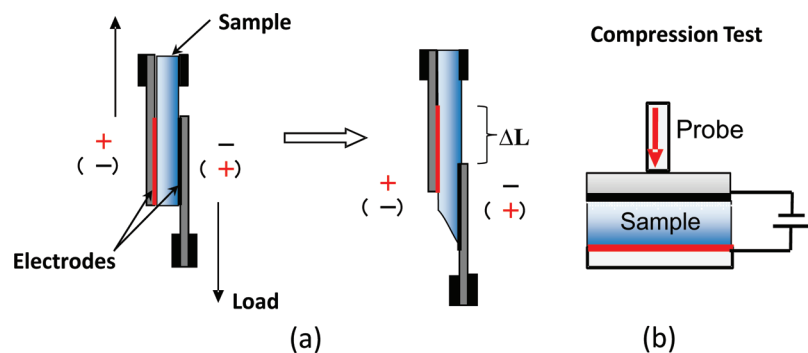


Figure 1. Two setups for (a) in situ shear tests and (b) compression experiments.

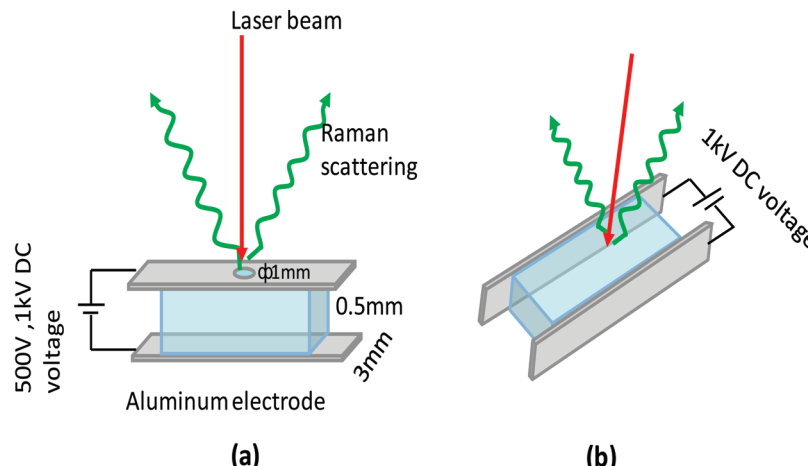


Figure 2. Raman scattering measurement for (a) gel surface and (b) gel cross section; in an electric field.

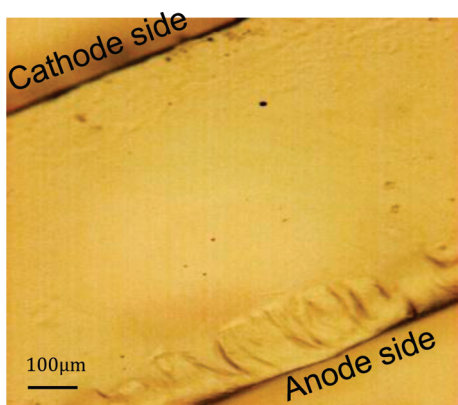


Figure 3. Microscope photographs of PVC gel in the cross section after application of an electric field.

interfacial shear strength due to the viscosity. Using this method, the deformation behavior of the gels with local layer structure can be evaluated. The displacement (ΔL) under increasing load represents the flexibility of the gel surface near one electrode.

2.3. FT-IR and Raman Spectroscopy. To clarify the influence of electric field intensity and polarity on PVC gels, we carried out attenuated total reflection Fourier transform infrared (ATR-FTIR) (Shimadzu Irprestige-21) and Raman spectroscopy (Kaiser HoloLab 5000 series, furnished with a 532 nm laser) on gel surfaces and/or cross sections under various applied DC electric fields. The gel was set between two electrodes either perpendicular or parallel to the laser beam, as shown in Figure 2. In Figure 2b, a hole ($\varphi = 1$ mm) was made in the top electrode for laser beam irradiation of the gel. Since the method of the attenuated total reflection (ATR) and surface scattering were used in FT-IR and Raman spectroscopy mea-

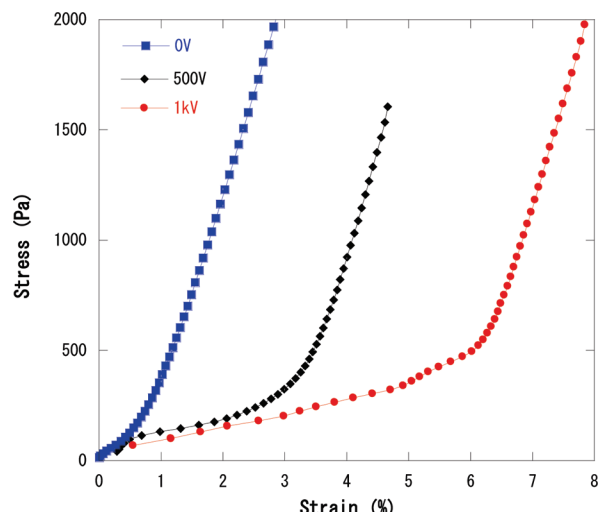


Figure 4. Stress-strain curves of PVC50 gel in compression mode.

surements, the surface ingredients of different samples and their variations near the anode or cathode can be evaluated.

3. Results and Discussion

3.1. Local Layer Structure of PVC Gel by Electrical Field. Figure 3 shows microscope images of the PVC gel in the cross section after application of an electric field. A layer structure appeared by a stepwise deformation due to the migration of the solvent-rich phase when an electrical field was applied to a uniform gel.^{18,20} The in situ compressive test with and without an applied electric field as shown in Figure 1a was used to investigate the compressive deformation behavior of the gels. Figure 4 shows stress-strain curves of PVC50 gel with and

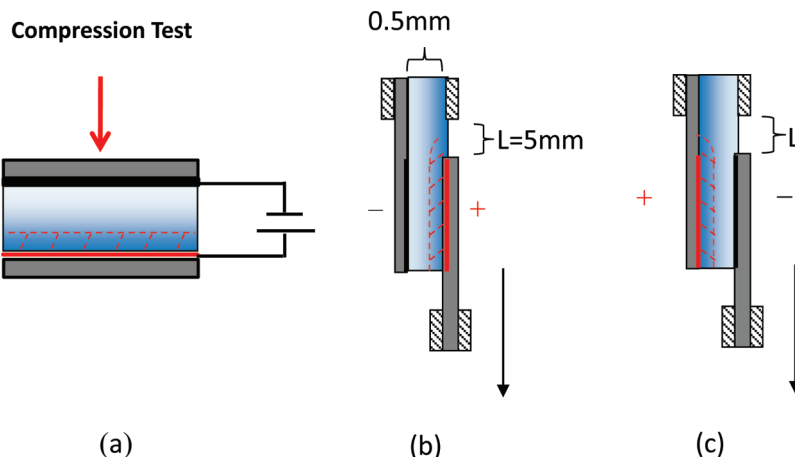


Figure 5. Schematic of the PVC gel layer separation in an electric field; in situ compression and shear deformation.

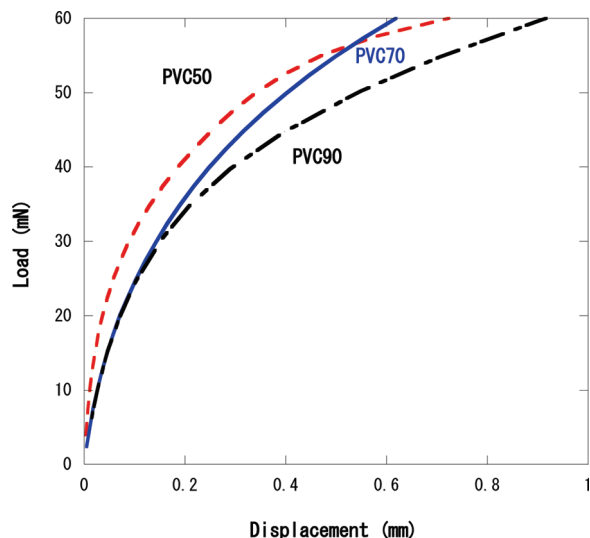


Figure 6. Load vs displacement plots for three PVC gel samples subjected to in situ shear stress.

without an electric field. In the absence of an applied electric field, an almost linear relationship between compressive stress and strain was observed, since the gel with 50 w/w% DBA was uniform. When an electric field of 500 or 1000 V was applied, the in situ stress-strain curves became two steps with an obvious knee point. The first linear parts of the curves were extended with increased electric field, which means that layer

separation progressed and the soft layer became thicker due to solvent-rich phase migration at larger DC power. It is considered that the extent of solvent-rich phase migration increased with increasing DC power. However, in the compressive test, the difference of actuation behavior near the anode or cathode could not be evaluated, because even when the electrodes are exchanged the mechanical deformation process is not changed (see Figure 5a).

3.2. Mechanical Properties near the Electrodes. To distinguish the difference of actuation behavior near the anode and cathode, the special shear test rig shown in Figure 5b and c was designed, in which shear deformation with local tension could be evaluated. For a material with more than two layers, neither a conventional shear test nor a tensile test can be used to investigate the contribution of individual layers. For a material such as PVC gel, deformed into a layer structure by an electric field, the dashed line area in Figure 5 represents a domain of electrical-field-induced layer separation. When one side of an electrode embedded in a part of the sample edge is pulled, a combination deformation with shear and tension in the area surrounding the electrode will occur. Thus, the local deformation behavior by an electric field can be evaluated when the electrode polarity is reversed.

Figures 6 and 7 show the results for gels with three different DBA contents, without and with applied DC voltage, obtained by this unique in situ combination test. The load-displacement behavior including both shear and local tensile deformations represents the actuation properties of the gel samples for the

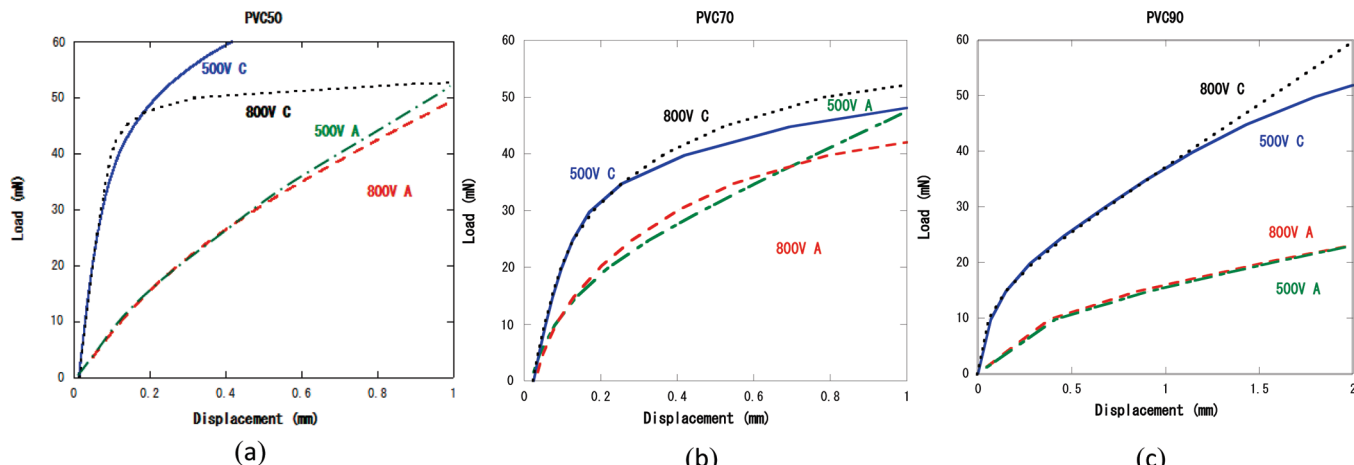


Figure 7. Comparison of the load-extension behavior of three PVC gels at the anode (A) and cathode (C) at a range of applied electric fields.

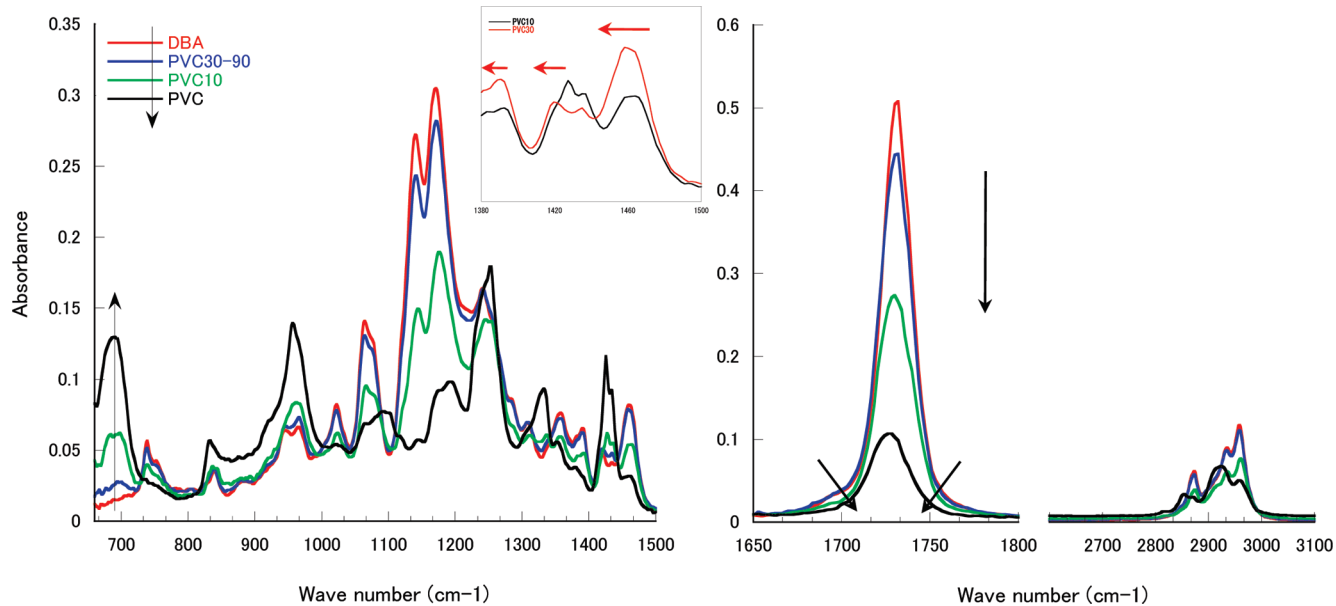


Figure 8. Comparison of the FT-IR spectra of all PVC gels, pure PVC film, and plasticizer (DBA). The inset shows the region between 1380 and 1500 cm^{-1} for PVC30 and PVC10, on an expanded scale.

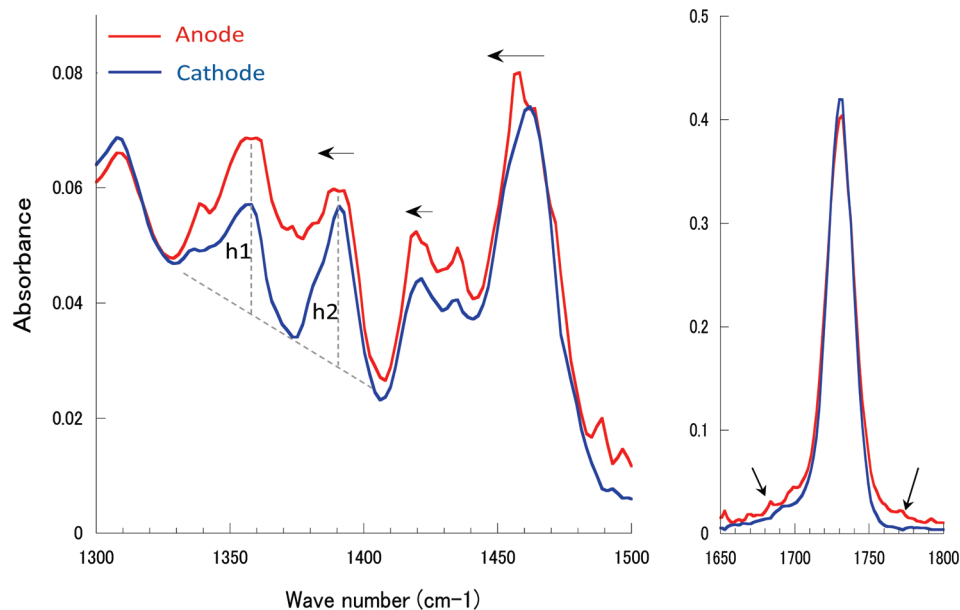


Figure 9. FT-IR spectra for PVC30 gel at the anode and cathode after application of a 2000 V mm^{-1} electric field.

case of electrode exchange. In the case of no applied DC power, the PVC gels become soft with an increase of DBA content. The slope of the load–displacement curve, i.e., the elastic modulus, clearly decreased for plasticizer DBA content more than 70 w/w%. When an electric field was applied (Figure 7), the load–displacement curves for all of the samples became quite different for anode and cathode pulling. In the case of anode pulling, the gels became more flexible, tenacious, and ductile than in the case of cathode pulling, since a local soft layer domain was formed near the anode. In particular, the curve for the PVC90 gel in anode pulling showed very easy deformation similar to uniform quasi-viscous flow.²² The elastic modulus of PVC gels in anode pulling was smaller than that in the absence of an applied electric field, and even much smaller than that in cathode pulling. These data provide clear evidence that the electric field power and the polarity of the electrodes have a great influence on PVC gel deformation due to the local layer structure. Moreover, when the electric power was changed from

500 to 800 V, for the same anode pulling, the load–displacement curves were almost the same in the initial deformation region. This was also the case for cathode pulling.

These results indicate that the electric field caused different gel deformation characteristics at the anode and cathode. It is considered that polymer-poor phases move to the anode and make the domain near the anode softer, and result in a layer structure. This may be one reason that creep in PVC gels always occurs along the anode when an electric field is applied.

The nonlinear part of the load–displacement curves also includes much information on PVC gel structure, such as cross-linking, chain entanglement status, effects on the fractal structure,²³ and so on. These aspects will be explored in future work.

3.3. FT-IR Analysis. Figure 8 shows FT-IR absorbance spectra of DBA, PVC10 gel, PVC30–90 gels, and PVC film. The characteristic peaks of PVC and DBA show large differences with variation of plasticizer content. The carbon–chlorine

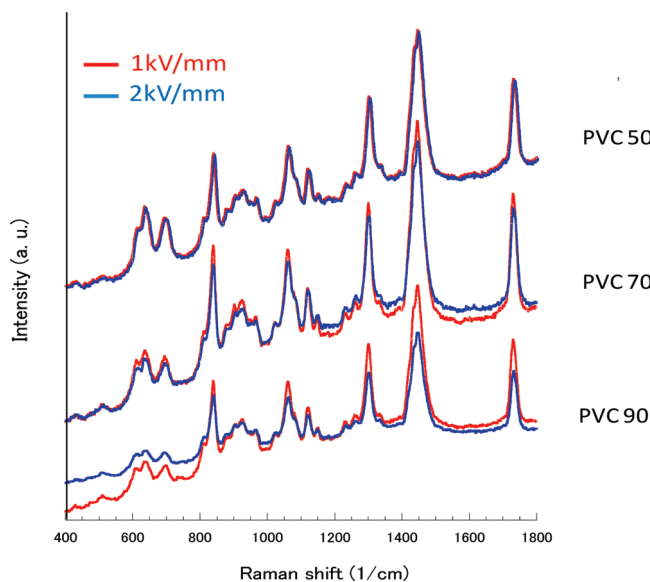


Figure 10. Raman spectra of PVC50, PVC70, and PVC90 gels in different electric fields.

(C—Cl) band is in the 700–760 cm^{-1} region, and the ester (C=O) stretching band is between 1700 and 1750 cm^{-1} .²⁴ The intensity of the C—Cl band increased, while the intensity and bandwidth of the ester (C=O) stretching band decreased with reduction of DBA content. PVC10 shows bands with intensity midway between those of DBA and PVC film. However, the spectra of the PVC gels with DBA content more than 30 w/w% are all similar to that of DBA, since there is a large proportion of DBA in these gels. The spectral comparison of PVC30 and PVC10 in the inset of Figure 8 shows that the peaks at 1385 and 1457 cm^{-1} were shifted to lower wavenumber when the DBA content increased from a low (PVC10) to a higher (PVC30) proportion.

On application of an electrical field, the PVC gels with high DBA content recover too rapidly; thus, we used the low DBA content specimen PVC30 to analyze the electric field effect at

the anode and cathode. In Figure 9, the $-\text{CH}_3$ symmetric band (1385 cm^{-1}) and $-\text{CH}_2$ scissoring band (1457 cm^{-1}) are dominant and they shifted to low wavenumber at the anode when 2000 V mm^{-1} was applied. This tendency is similar to the peak shift that occurred (inset of Figure 8) when the DBA content was changed. Furthermore, the absorbance ratio ($h1/h2$) of the 1358 and 1390 cm^{-1} bands is about 1 at the anode and 0.6 at the cathode. Also, several small waves are observed in the vicinity of the ester (C=O) stretching band, and the C=O bandwidth was increased at the anode. These differences between the anode and cathode in FT-IR analysis are considered as that the concentration of DBA was changed due to the solvent-rich phase migration when an electric field was applied to PVC gels.

3.4. Raman Spectra. Raman spectroscopy is complementary to FT-IR spectroscopy^{24,25} and can detect variation of molecular polarizability during in situ application of the electric field.^{26–28} In Figure 10, the spectra (obtained using the method shown in Figure 2a) of three samples (PVC50, PVC70, and PVC90 gels) with 1 and 2 kV mm^{-1} electric fields are shown. Peak shifts were not observed, but the intensity of the whole spectrum changed with the changing DC power. It may be assumed that the Raman spectra contain information related to gel deformation. For the PVC50 gel, no apparent change in the intensity of the bands was observed when the electric field was increased from 1 to 2 kV mm^{-1} , since PVC50 gel was the hardest of the three samples, and more difficult to deform than the other two gels. However, the PVC70 and PVC90 gels showed the whole intensity of spectrum changes at different applied electric fields. The intensity of the spectrum also depended on the content of DBA. The higher the electric power, corresponding to higher stress, the larger strain, resulting in lower intensity of the Raman spectrum.

Since the electrodes may limit the direction of gel deformation, the method shown in Figure 2b was employed to measure deformation characteristics of PVC gel cross sections. The results are shown in Figure 11: the Raman spectra were obtained at five laser irradiation positions in the cross section, with (a) 0 V and (b) 2000 V mm^{-1} of DC electric power. There were no

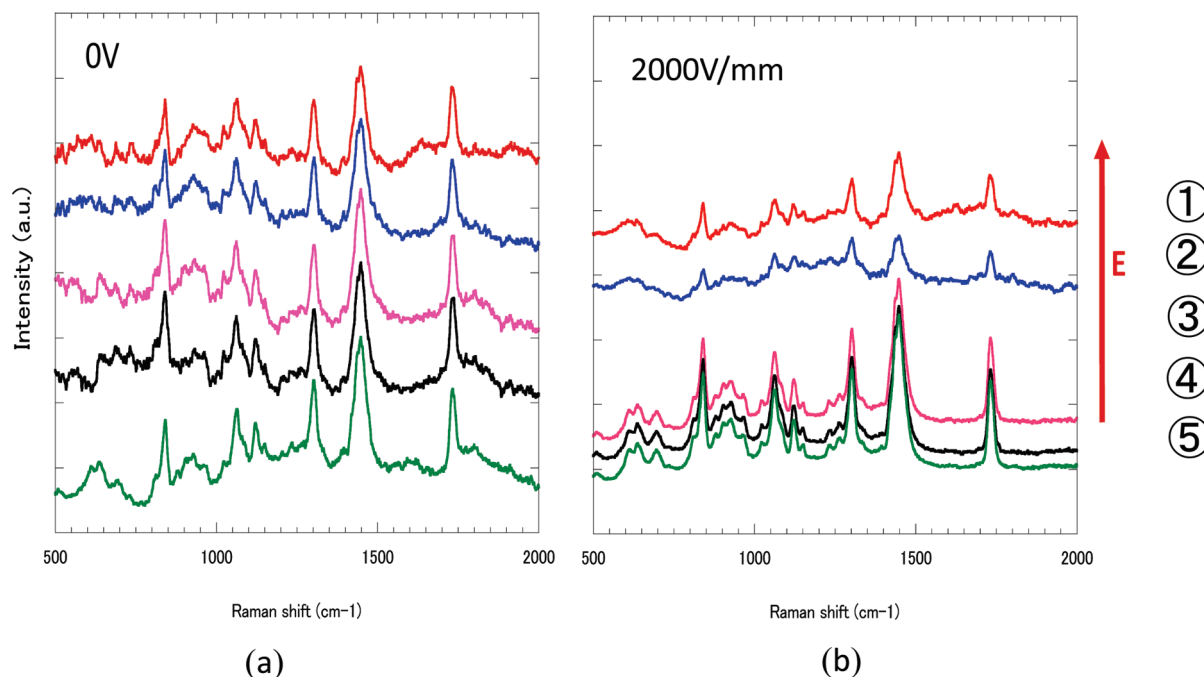


Figure 11. Raman spectra of the cross section of PVC90 gel without (a) and with a 2000 V mm^{-1} electric field (b).

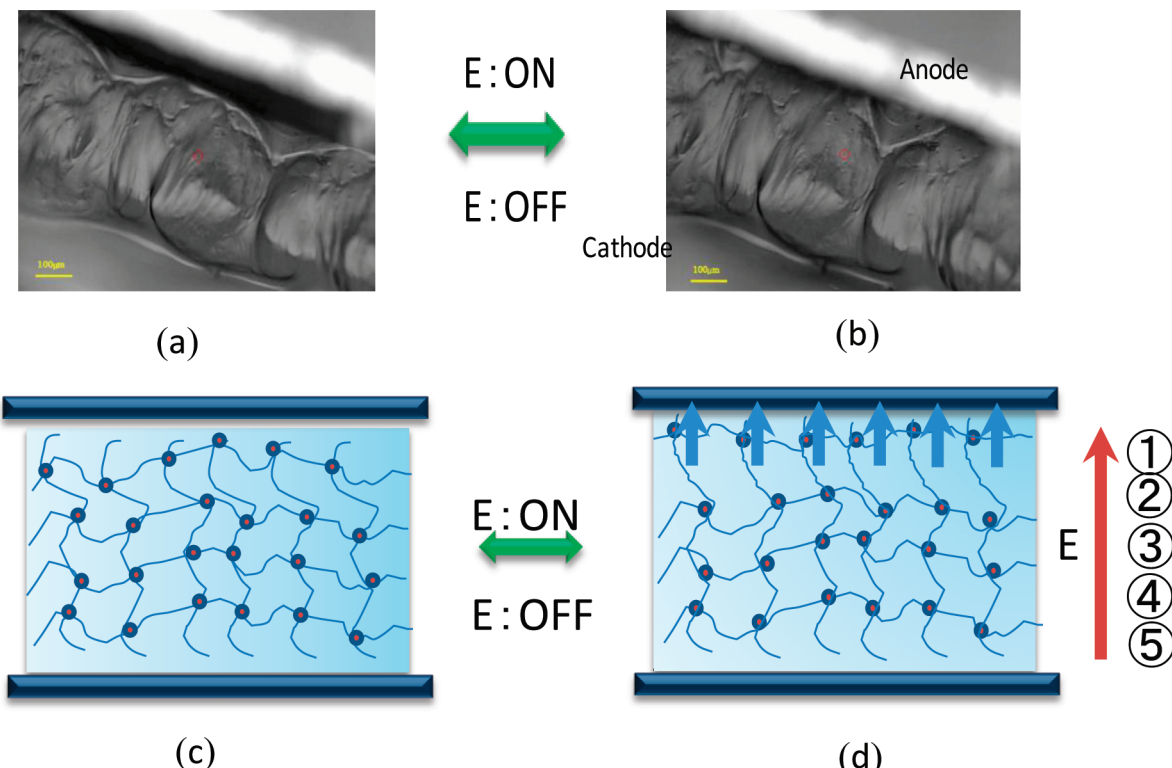


Figure 12. (a and b) Microscopic images of PVC gel in Raman spectral analysis; the red circle is the point of laser irradiation. (c and d) Model of electric-field-induced strain in gel microstructure.

large variations without applied DC voltage. When 2000 V mm^{-1} of electric power was applied, damped spectra appeared near the anode, which means that a large distortion was generated near the anode. The spectra in the middle position and cathode are similar to Figure 11a, and there was no significant distortion. In addition, microscope images showed the actual state of the gels during Raman measurement (see Figure 12a and b). The strain pattern induced by the attractive force from the anode was obtained while the electric field was applied (see Figure 12b). The reason may be that the PVC gel network was extended by stress, and the distance between the cross-link points increased upon increasing the electric field as represented in the imaging models of Figure 12c and d. This damping effect of electric-field-induced Raman scattering intensity, with reduction in intensity of spectrum peaks, may be related to phonon–hole scattering due to the strong interaction between the phonons and the photogenerated hole carriers.^{29–31} The Raman spectra at five positions from the anode to the cathode were definitely different, especially near the anode and cathode. This variation also supports the different deformation behavior from the anode to the cathode due to the electric-field-induced solvent-rich phase moving to the anode.

4. Conclusions

Using Fourier transform infrared (FT-IR) spectrometry, in situ Raman spectroscopy, and a combined shear and compression test, we successfully clarified the electric-field-induced local layer structure and the migration of the solvent-rich phase in PVC gels. The layer of PVC gel clinging to the anode is softer than that near the cathode. The technique of combined shear and compression test is proposed to obtain the mechanical properties of PVC gel in the anode and cathode during applied electric field, and this is a powerful method in the studies of actuator materials including the PVC gels. The peaks of FT-IR

spectra were shifted (at 1385 and 1457 cm^{-1}) and changed (between 1700 and 1750 cm^{-1}) in the gel surface near the anode from the cathode. By the in situ Raman spectroscopy, it is found that the intensity of whole Raman spectra were reduced from the cathode to anode, and the elastic modulus of the gel on the anode was smaller than that on the cathode. All of the results were in good agreement to indicate that the electric field induced the increment of the polymer-poor phase and caused a larger deformation in the PVC gels near the anode. This maybe is one reason that stimulation of creep always occurs along the anode of PVC gel actuators when an electric field is applied.

Acknowledgment. This work was partially supported by a Grant-in-Aid for Global COE Program by the Ministry of Education, Culture, Sports, Science, and Technology.

References and Notes

- (1) Aoki, Y. *Macromolecules* **2001**, *34*, 3500–3502.
- (2) Girard-Reydet, E.; Pascault, J. P. *Macromolecules* **2000**, *33*, 3084–3091.
- (3) Li, L.; Uchida, H.; Aoki, Y. *Macromolecules* **1997**, *30*, 7842–7848.
- (4) Marcilla, A.; Garcia-Quesada, J. C.; Gil, E. *J. Appl. Polym. Sci.* **2008**, *110* (4), 2102–2107.
- (5) Boudhani, H.; Laine, C.; Fulchiron, R.; Cassagnau, P. *Rheol. Acta* **2007**, *46*, 825–838.
- (6) Pielichowski, K. *Eur. Polym. J.* **1999**, *35*, 27–34.
- (7) Guenet, J. *Thermoreversible gelation of polymers and biopolymers*; Academic Press: London, 1992.
- (8) Wu, C.; Zhou, S. *Macromolecules* **1997**, *5* (2), 114–119.
- (9) Bair, H. E.; Matsuo, M.; Salmon, W. A.; Kwei, T. K. *Macromolecules* **1972**, *30*, 574–576.
- (10) Aoki, Y.; Li, L.; Uchida, H.; Kakiuchi, M. *Macromolecules* **1998**, *31*, 7472–7478.
- (11) Li, L.; Aoki, Y. *Macromolecules* **1998**, *31*, 740–745.
- (12) Watanabe, H.; Sato, T.; Osaki, K.; Aoki, Y.; Li, L.; Kakiuchi, M.; Yao, M.-L. *Macromolecules* **1998**, *31*, 4198–4204.
- (13) Hong, P.-D.; Chou, C.-M. *Macromolecules* **2000**, *33*, 9673–9681.
- (14) Uddin, Md. Z.; Watanabe, M.; Shirai, H.; Hirai, T. *J. Rob. Mechatronics* **2002**, *14* (2), 118–123.

- (15) Uddin, Md. Z.; Yamaguchi, M.; Watanabe, M.; Shirai, H.; Hirai, T. *Chem. Lett.* **2001**, *30* (4), 360–361.
- (16) Hirai, T.; Ogiwara, T.; Fujii, K.; Ueki, T.; Kinoshita, K.; Takasaki, M. *Adv. Mater.* **2009**, *21*, 2886–2888.
- (17) Hirai, T.; Kobayashi, S.; Hirai, M.; Yamaguchi, M.; Uddin, Md. Z.; Watanabe, M.; Shirai, H. *Proc. SPIE* **2004**, *5385*, 433–441.
- (18) Xia, H.; Takasaki, M.; Hirai, T. *Sens. Actuators, A* **2010**, *157*, 307–312.
- (19) Xia, H.; Hirai, T. *Proc. IEEE ICMA* **2009**, *16*, 4–169.
- (20) Xia, H.; Ueki, T.; Hirai, T. *Adv. Mater. Res.* **2009**, *79–82*, 2063–2066.
- (21) Hirai, T.; Ueki, T.; Takasaki, M. *JFB* **2008**, *1* (1), 1–6.
- (22) Masaki, S. *Polymer materials*; The micromolecule engineering series 4; Nikan Industrial Newspaper Publishing Co.: Tokyo, 1975.
- (23) van Krevelen, D. W.; Te Nijenhuis, K. *Properties of Polymers: Their Correlation with Chemical Structure; Their Numerical Estimation and Prediction from Additive Group Contributions*, 4th ed.; Elsevier: Oxford, U.K., 2009.
- (24) Hesse, M.; Meier, H.; Zeeh, B. *Spectroscopic methods in organic chemistry*; Kagakudojin: Kyoto, 2000.
- (25) Kitagawa, T.; Tu, A. T. *Introduction to Raman Spectroscopy*; Kagakudojin: Kyoto, 1988.
- (26) Cavicchioli, A.; de Faria, D. L. A. *Sens. Actuators, B* **2006**, *115*, 656–665.
- (27) Han, H.-S.; Kang, H.-R.; Kim, S.-W.; Kim, H.-T. *J. Power Sources* **2002**, *112*, 461–468.
- (28) Chung, J. W.; Kim, S. H.; Jung, S. J.; Kwak, S.-Y. *Eur. Polym. J.* **2009**, *45*, 2164–2171.
- (29) Sarua, A.; Ji, H.; Kuball, M. *Appl. Phys. Lett.* **2006**, *88*, 103502.
- (30) Hussain, A.; Ahn, C. W.; Lee, J. S.; Ullah, A.; Kim, I. W. *Sens. Actuators, A* **2010**, *158*, 84–89.
- (31) Jeong, T. S.; Youn, C. J.; Han, M. S.; Yang, J. W.; Lim, K. Y. *Appl. Phys. Lett.* **2003**, *83* (17), 3483–3485.

JP105239A